

## Stacked $\pi$ -type Equivalent Circuit Analysis of Ferromagnetic RF Integrated Inductor

Masahiro Yamaguchi, Shinji Ikeda, Seok Bae, Shinji Tanabe<sup>1</sup>, Kengo Sugawara<sup>1</sup> and Adalbert Konrad<sup>2</sup>

Tohoku University, Department. of Electrical and Communication Engineering  
05 Aramaki-aza-Aoba, Aoba-ku, Sendai, Miyagi 980-8579, Japan

Phone: +81-22-217-7077, FAX: +81-22-263-9410, E-mail: yamaguti@ecei.tohoku.ac.jp

<sup>1</sup>Mitsubishi Electric Corporation, Advanced Technology R&D Center  
8-1-1 Tsukaguchi-Honmachi, Amagasaki, 661-8661, Japan

<sup>2</sup>University of Toronto, Department of Electrical and Computer Engineering  
Toronto, ON, M5S 3G4, Canada

### 1. Introduction

It is becoming realistic to apply soft magnetic thin films on the top of RF integrated spiral inductors [1], [2] with the development of RF soft magnetic films [3], [4]. It is useful for the design and analysis of the Q-value and self-resonance of the inductors to use an equivalent circuit.

Last year we have proposed a stacked- $\pi$  type equivalent circuit for a ferromagnetic RF spiral inductor with magnetic film on top of the spiral, followed by the low frequency approximation of the proposed equivalent circuit to ease parameter extraction up to 5 GHz [5], [6].

In this paper, we eliminated the low frequency approximation and extracted all the stacked- $\pi$  type equivalent circuit parameters of the inductor by introducing an appropriate cost function to fit the measured frequency profile of the impedance of the inductor up to 12 GHz. This greatly helped to estimate the influence of parasitic impedance associated with the magnetic film.

### 2. Structure and Fabrication Process

Fig. 1 illustrates a two-port type ferromagnetic RF integrated spiral inductor studied in this work [5]. The coil is made of 2.6- $\mu\text{m}$ -thick Cu with line width of 12  $\mu\text{m}$  and line spacing of 10  $\mu\text{m}$ . The outer size of the square spiral is 393 $\times$ 393  $\mu\text{m}^2$ . A 0.1- $\mu\text{m}$ -thick anisotropic soft ferromagnetic amorphous  $\text{Co}_{85}\text{Nb}_{12}\text{Zr}_3$  (atomic %) film was sputter deposited on top of the coil with a 3.2- $\mu\text{m}$

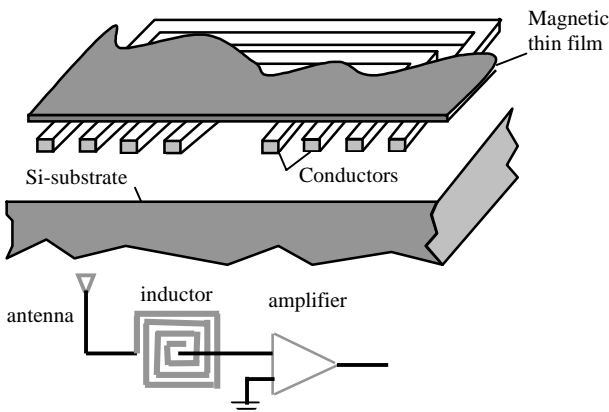


Fig.1 Spiral inductor with magnetic film used in matching circuit.

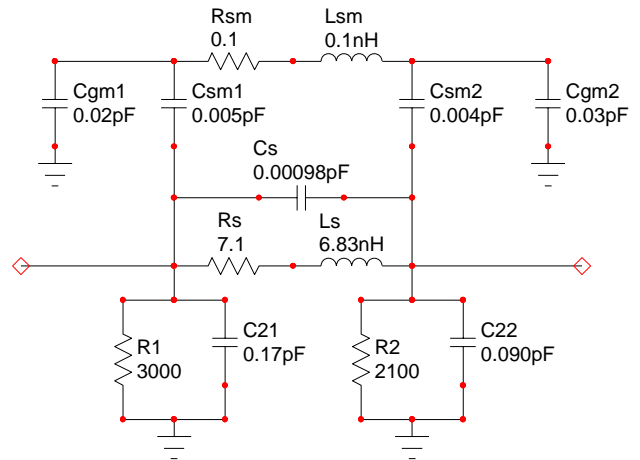


Fig.2 - Result of fitting for an inductor.

thick polyimide insulator layer in between. The processing substrate was n-type (100) Si with  $\rho > 500 \Omega\text{cm}$ .

### 3. Equivalent Circuit Description

Fig. 2 shows the structure of the proposed stacked- $\pi$  type equivalent circuit. Main components of the inductor are the series connection of  $L_s$  and  $R_s$ , representing the contribution of air core spiral and ferromagnetic thin film. The connection of  $L_s$ ,  $R_s$ ,  $R_1$ ,  $R_2$ ,  $C_{21}$ ,  $C_{22}$  and  $C_s$  exhibits the first  $\pi$  type equivalent circuit of an RF integrated inductor while another components form the second  $\pi$  type circuit which represents parasitic impedances associated with the magnetic film.

A network analyzer (HP 8720D) was used together with two G-S-G type wafer probes (Pico Probe, GGB Industries, Inc.) to measure S-parameters. Then the S-parameters were converted into Z-parameters with one-to-one correlation. Fig. 3 and Fig. 4 show these results. It is a feature of this work to use Z-parameters instead of S-parameters as the fitting target of the cost function to extract the equivalent circuit parameters. This is because the Z-parameters exhibited sharp peaks and dips in the frequency profile and this eased much the convergence of the cost function.

Such a sharp change of Z-parameter also suggests to use the logarithm of  $|Z|$  rather than linear function of  $|Z|$  for the cost function.

cost function

$$= \sum_{\omega, m, n} \left| \log \{ Z_{mn}^{meas.}(\omega) \} - \log \{ Z_{mn}^{equi. circuit}(\omega, R_s, L_s, \dots R_{sm}) \} \right|^2 \quad (1)$$

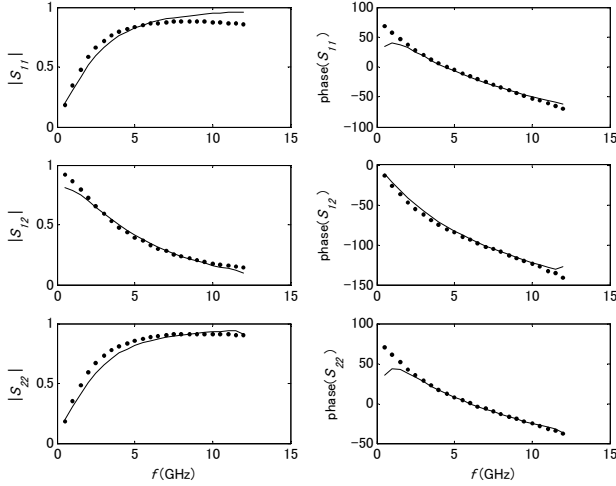


Fig.4 Fitting using S-parameters. The dots are measured values.

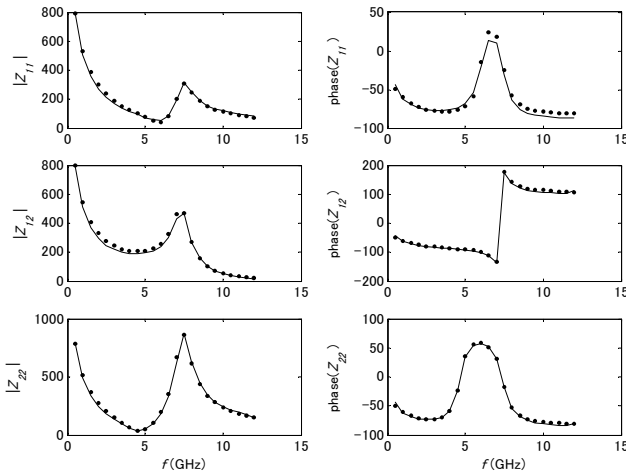


Fig.5 - Fitting using Z-parameters. The dots are measured values.

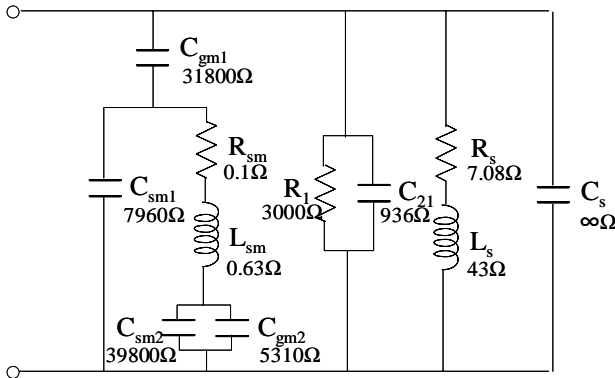


Fig.6 Equivalent Circuit for shorted output at 1GHz.

### 3. Discussion

Extracted equivalent circuit parameters are shown in Fig. 2. The values of  $L_s=6.83\text{nH}$  and  $R_s=7.1\Omega$  nominally leads  $Q=6.0$  at  $f=1\text{ GHz}$ . The substrate resistances are  $R_1=3000\Omega$  and  $R_2=2100\Omega$ , which are much higher than the supposed system impedance of  $50\Omega$  and therefore the substrate losses should be negligible. This is a benefit of using high resistivity Si wafer.

To discuss the parasitic impedance in detail, reactance at 1GHz are calculated as shown in Fig. 6. The output port (right hand side port in Fig. 2) is short circuited to define input impedance of the inductor. It is seen that the impedance of the stray capacitances of the second  $\pi$  type circuit are much higher than other components and therefore the Q-value will depend only on the spiral inductance,  $L_s$ , resistance,  $R_s$ , and the parasitics,  $R_1$  and  $C_{21}$ , between the coil and ground via Si substrate.

If the supposed drive frequency is raised to 10 GHz, impedance of the stray capacitances in the second  $\pi$  type circuit will be only one order higher than that of the main inductance and therefore those significantly degrade the performance of the inductor.

### Conclusion

Extraction of the stacked- $\pi$  type equivalent parameters for a ferromagnetic RF integrated inductor has been demonstrated. It is useful to employ Z-parameters as the fitting target of the cost function to extract the parameters due to sharp peaks and dips in the frequency profile. Accurate Q-factor extraction became possible through this analysis. Parasitic impedance of magnetic film is negligible at 1 GHz but degrades the performance at 10 GHz in case of the  $393 \times 393\text{ }\mu\text{m}^2$  size on-top type ferromagnetic RF integrated inductor.

This work is supported partly by Grant-in-Aid for Scientific Research Priority Areas (A), Highly Functionized Global Interface Integration, No. 13025202.

### References

- [1] M. Yamaguchi, K. Suezawa, K. I. Arai, Y. Takahashi, S. Kikuchi, Y. Shimada, W. D. Li, S. Tanabe, and K. Ito, J. Appl. Phys., Vol. 85, pp. 7919-7922 (1999).
- [2] S. Tanabe, Y. Shiraki, K. Itoh, M. Yamaguchi and K. I. Arai, IEEE Trans. Magn., Vol. 35, No. 5, pp3580-3582 (1999)
- [3] K. Katoh, W. D. Li, O. Kitakami and Y. Shimada, J. of Magnetism Society of Japan, Vol. 21, No. S2, pp. 423-428 (1997)
- [4] S. Ohmura, N. Kobayashi, T. Masumoto and H. Fujimori, J. of Magnetism Society of Japan, Vol. 22, pp. 441-444 (1998)
- [5] T. Kuribara, M. Yamaguchi, and K. Arai, IEEE Trans. Magn., Vol.38, No.5, pp.3159-3161, Sept. 2002.
- [6] M. Yamaguchi, Y. Yokoyama, S. Ikeda, T. Kuribara, K. Masu and K. I. Arai, Jpn.J.Appl.Phys. Vol.42, Part 1, No.4B, pp. 2210–2213 (2003).
- [7] A. Konrad, S. Tanabe, R. Jafari, K. Sugahara and M. Yamaguchi, Intermag '03, FC-06 (2003).